15

Role of Biomechanical Parameters in Hip Osteoarthritis and Avascular Necrosis of Femoral Head

Veronika Kralj - Iglič[1], Drago Dolinar[1], Matic Ivanovski[1], Ivo List[1] and Matej Daniel[2]
[1]*Laboratory of Clinical Biophysics, Faculty of Medicine, University of Ljubljana*
[2]*Laboratory of Biomechanics, Faculty of Mechanical Engineering, Technical University in Prague*
[1]*Slovenia*
[2]*Czech Republic*

1. Introduction

It is considered that living organisms are subject to physical laws. Forces and stresses importantly influence the development of tissues and cells. In order to manipulate physiological and patophysiological states of the organism, it is necessary to understand the underlying mechanisms. Experience has led to mechanical hypothesis stating that some diseases or disorders are a consequence of unfavorable load distribution which is expressed by biomechanical parameters (e.g. forces, stresses, load - bearing areas). Since 1993 we have considered contact stress in the hip joint. We took part in development of a mathematical model for determination of the contact hip stress distribution (Iglič (1993b); Ipavec (1999)) and in population studies which were performed to validate the model. Different diseases and disorders of the hip were considered by this model: hip dysplasia (Mavčič (2002; 2008); Pompe (2003; 2007)), slipped epiphysis of the femoral head (Zupanc (2008)), avascular necrosis of the femoral head (Daniel (2006); Dolinar (2003)), postoperative changes in hip geometry (Herman (2002); Kralj (2005); Vengust (2001)) and osteoarthritis of the hip (Rečnik (2007; 2009a;b)). The method HIPSTRESS was put forward consisting of mathematical model for resultant hip force (Iglič (1990; 1993a)), mathematical model for contact hip stress (Iglič (1993b); Ipavec (1999)) and the corresponding software. The models require as an input geometrical parameters of the hip and pelvis. These parameters can be assessed from images as for example from standard anteroposterior radiograms. As appropriate images are available from clinical practice and from the archives, prospective and retrospective studies of the development of different diseases can be performed. A thorough survey on resultant hip force and the corresponding stress has recently been published (Daniel (2011)).

Albeit the HIPSTRESS method is of limited repeatability and accuracy, the population studies have shown that biomechanical parameters are useful in reaching better understanding of

mechanisms taking place in different diseases and in predicting the outcome of the treatment, on the level of populations. In particular, the results indicated that long lasting elevated contact stress is connected to degeneration of the hip articular cartilage and development of hip osteoarthritis (Dolinar (2003); Kralj (2005); Mavčič (2002; 2008); Pompe (2003); Rečnik (2007; 2009a;b)).

The physical content of the model for hip stress used in these studies is simple and clear. The model states that the resultant hip force is distributed over the load - bearing area according to the corresponding normal stress in the cartilage which is subject to Hooke's law. The equations that must be solved to obtain the relevant forces, stresses and load - bearing area are transparent while the solution of the problem is almost analytical. Moreover, a user - friendly software HIPSTRESS was developed which by fast determination of biomechanical parameters of the hip and pelvis enables analyses of large populations of hips.

However, due to space limitations in journals, the full derivation of the model equations was not encouraged in our previously published papers. Presenting only the final short and elegant equation for determination of stress parameters may lead the readers to think that the model itself is also simple. To elucidate the derivation and the model assumptions, we present in the first part of this work a detailed derivation of the model for contact hip stress distribution within the HIPSTRESS method, and indicate the connection between an unfavorable stress distribution and osteoarthritis development. In the second part, we present new results indicating the contact hip stress distribution as an etiological factor in avascular necrosis of the femoral head.

2. Determination of hip stress distribution by mathematical model

The femoral head is represented by a fraction of a sphere (the femoral head sphere) and the acetabulum is represented by a half of a spherical shell (the acetabular sphere). An articular spherical surface is imagined. This spherical surface is an abstract object rather than a physical one and extends beyond the load - bearing area. The load - bearing area is however a part of the articular spherical surface.

The shear stresses in the hip joint are neglected because of the small value of the frictional coefficient corresponding to forces acting in the hip joint (Eberhardt (1991); Lipshitz (1979); McCutchen (1962)) so that only the normal stress is considered. We refer to the normal stress as to the contact hip stress.

When the hip is unloaded, the femoral head sphere and the acetabular sphere are concentric (Fig.1A). Upon loading the femoral head moves towards the acetabulum thereby squeezing the cartilage in between (Fig.1B). The femoral head sphere and the acetabular sphere are no longer concentric and the surfaces are shifted with respect to each other. The point on the articular sphere corresponding to the closest approach of the femoral head sphere and the acetabular sphere is called the stress pole (denoted by P in Fig.1B).

The radius vector from the centre of the femoral head sphere to the selected point at the acetabular sphere after the loading is denoted by $\mathbf{r}$, the respective radius vector before the loading is denoted by $\mathbf{r}'$ and the penetration of the centre of the femoral head is denoted by $\mathbf{d}$. The coordinate system is rotated so that the side view plane is defined by the three vectors.

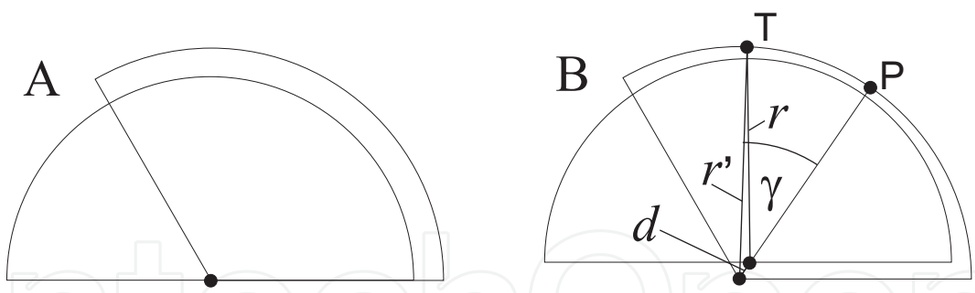

Fig. 1. Schematic presentation of the relative shift of the acetabular sphere and the femoral head sphere. A: before loading, the two spheres are concentric. B: after loading, the femoral head sphere penetrates towards the acetabular sphere.

It follows from trigonometric relations that

$$r^2 = r'^2 + d^2 - 2r'd\cos\gamma \tag{1}$$

where γ (Fig. 1B) is the angle between the radius vector from the origin of the coordinate system at the centre of the articular sphere to the pole and the radius vector to the selected point on the articular surface while r, r' and d are the magnitudes of the vectors $\mathbf{r}$, $\mathbf{r}'$ and $\mathbf{d}$. It is considered that the deformation of the cartilage is very small i.e. that the distance of penetration d is much smaller than distances r and r', so we can neglect the quadratic term in Eq.(1),

$$r = \sqrt{r'^2 - 2r'd\cos\gamma} \tag{2}$$

and use the approximation for small x, $\sqrt{1+x} \simeq 1 + x/2$,

$$r = r'(1 - \cos\gamma\frac{d}{r'}). \tag{3}$$

The deformation and the strain of the cartilage are proportional to the difference $r' - r$,

$$r' - r = d\cos\gamma. \tag{4}$$

As the normal stress at a particular point on the articular sphere (p) is taken proportional to strain in the cartilage, it can be written as (Brinckmann (1981))

$$p = p_0\cos\gamma \tag{5}$$

where the proportionality constant p_0 is the value of stress at the pole.

Considering the resultant hip force $\mathbf{R}$ to be known, it is connected to the hip stress distribution by

$$\int p_0\cos\gamma\mathbf{dS} = \mathbf{R}, \tag{6}$$

where $\mathbf{dS}$ is the vector form of the area element pointing in the direction normal to the surface. The integration is performed over the load - bearing area.

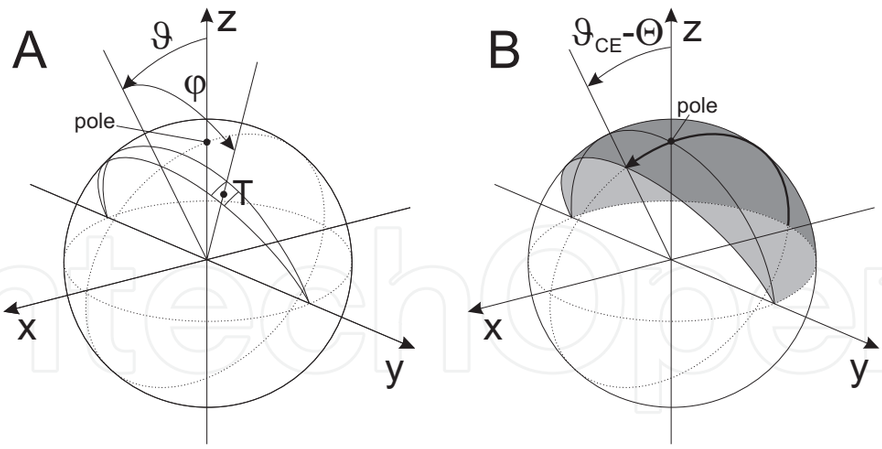

Fig. 2. Schematic presentation of the articular sphere and the coordinate system.

The coordinate system is adjusted to the geometry of the load-bearing area. The coordinates of a selected point (T) are (Fig.2A)

$$x = r\cos\varphi\sin\vartheta, \tag{7}$$

$$y = r\sin\varphi, \tag{8}$$

$$z = r\cos\varphi\cos\vartheta. \tag{9}$$

The infinitesimal element of the surface area is given by

$$\mathbf{dS} = r^2\cos\varphi(\cos\varphi\sin\vartheta, \sin\varphi, \cos\varphi\cos\vartheta)\mathrm{d}\varphi\mathrm{d}\vartheta. \tag{10}$$

The space angle γ is the angle between the radius vector to the stress pole and the radius vector to the selected point on the articular surface, hence we can use the dot product to define the angle,

$$\cos\gamma = \frac{\mathbf{r}\cdot\mathbf{r}_{\mathrm{pole}}}{r^2}, \tag{11}$$

where

$$\mathbf{r} = r(\sin\vartheta\cos\varphi, \sin\varphi, \cos\vartheta\cos\varphi), \tag{12}$$

and

$$\mathbf{r}_{\mathrm{pole}} = r(\sin\Theta\cos\Phi, \sin\Phi, \cos\Theta\cos\Phi). \tag{13}$$

The dot product yields

$$\mathbf{r}\cdot\mathbf{r}_{\mathrm{pole}} = r^2(\sin\vartheta\cos\varphi\sin\Theta\cos\Phi + \sin\varphi\sin\Phi + \cos\vartheta\cos\varphi\cos\Theta\cos\Phi) \tag{14}$$

so that

$$\cos\gamma = \sin\vartheta\cos\varphi\sin\Theta\cos\Phi + \sin\varphi\sin\Phi + \cos\vartheta\cos\varphi\cos\Theta\cos\Phi. \tag{15}$$

In the chosen coordinate system, the position of the pole is given by two angles (Φ and Θ). However, for clarity and simplicity we rotate the hip in the coordinate system so that the pole is at the top of the articular sphere (Fig.2B),

$$\cos\tilde{\Theta} = 1, \tag{16}$$

and

$$\sin\tilde{\Theta} = 0, \tag{17}$$

while $\tilde{\Phi} = 0$ so that

$$\cos\tilde{\Phi} = 1, \tag{18}$$

and

$$\sin\tilde{\Phi} = 0. \tag{19}$$

It follows from Eqs.(15) and (16)– (19) that in the rotated system

$$\cos\gamma = \cos\varphi\cos\vartheta. \tag{20}$$

2.1 Contact hip stress in relation to resultant hip force

Using expressions (5), (6), (10) and (20), the components of the vector equation for the resultant hip force in the rotated system are expressed as

$$R_x = p_0 r^2 \int \cos^3\varphi \mathrm{d}\varphi \int \cos\vartheta \sin\vartheta \mathrm{d}\vartheta, \tag{21}$$

$$R_y = p_0 r^2 \int \cos^2\varphi \sin\varphi \mathrm{d}\varphi \int \cos\vartheta \mathrm{d}\vartheta, \tag{22}$$

$$R_z = p_0 r^2 \int \cos^3\varphi \mathrm{d}\varphi \int \cos^2\vartheta \mathrm{d}\vartheta. \tag{23}$$

In order to calculate the coordinates of the pole Θ and Φ and the value of stress at the pole p_0 we must solve the above system of equations. For this we must define the boundaries of the load - bearing area within the articular surface.

We take for simplicity that the lateral border of the load - bearing area is defined by the lateral rim of the acetabulum. Neglecting the detailed anatomy of the border and taking that the rim presents a part of a circle on the sphere with the centre at the centre of the sphere, the rim is described by an intersection of the articular sphere and a plane passing through the center of the sphere. The plane is inclined by an angle ϑ_{L} with respect to the vertical axis. The coordinate system is then rotated for an angle $-\Phi$ so that the lateral border is symmetric with respect to the frontal plane through the centre of the articular sphere. Stress represents loading only if it is positive. Therefore the medial border of the load - bearing area is defined at points on the articular sphere where stress vanishes,

$$\cos\gamma = 0. \tag{24}$$

This condition includes points which are for $\pi/2$ away from the stress pole.

Consider a hip with the lateral coverage ϑ_{L} and the pole of stress (given by angles Θ and Φ) located laterally with respect to the sagittal plane through the centre of the femoral head. The coordinate system is rotated for angles $-\Theta$ and $-\Phi$, so in the rotated system, the lateral border is at $\vartheta = \vartheta_{\mathrm{L}} - \Theta$. As the pole is at the top of the rotated system, the medial border in the rotated system is at $\vartheta = -\pi/2$. Parameter φ is bounded within the interval $[-\pi/2, \pi/2]$.

Taking into account that

$$\int \cos^3 \varphi \mathrm{d}\varphi = \sin \varphi - \frac{1}{3} \sin^3 \varphi, \tag{25}$$

$$\int \cos \vartheta \sin \vartheta \mathrm{d}\vartheta = \frac{1}{2} \sin^2 \vartheta, \tag{26}$$

$$\int \cos^2 \varphi \sin \varphi \mathrm{d}\varphi = -\frac{1}{3} \cos^3 \varphi, \tag{27}$$

$$\int \cos \vartheta \mathrm{d}\vartheta = \sin \vartheta, \tag{28}$$

$$\int \cos^2 \vartheta \mathrm{d}\vartheta = \frac{1}{2}(\vartheta + \frac{1}{2} \sin 2\vartheta), \tag{29}$$

and considering the boundaries, the components of the force are

$$R_x = -p_0 r^2 \frac{2}{3} \cos^2(\vartheta_\mathrm{L} - \Theta) \tag{30}$$

$$R_y = 0 \tag{31}$$

and

$$R_z = p_0 r^2 \frac{2}{3}(\vartheta_\mathrm{L} - \Theta + \frac{\pi}{2} + \frac{1}{2} \sin 2(\vartheta_\mathrm{L} - \Theta)). \tag{32}$$

The resultant hip force is given by the vector

$$\mathbf{R} = R(-\sin \vartheta_R \cos \varphi_R, \sin \varphi_R, \cos \vartheta_R \cos \varphi_R) \tag{33}$$

which is in the rotated system expressed as

$$\mathbf{R} = R(-\sin(\vartheta_R + \Theta), 0, \cos(\vartheta_R + \Theta)) \tag{34}$$

since

$$\Phi = -\varphi_R. \tag{35}$$

The ratio R_x/R_z yields

$$\tan(\vartheta_R + \Theta) = \frac{\cos^2(\vartheta_\mathrm{L} - \Theta)}{(\vartheta_\mathrm{L} - \Theta + \frac{\pi}{2} + \frac{1}{2} \sin 2(\vartheta_\mathrm{L} - \Theta))}. \tag{36}$$

Eq.(36) is a nonlinear equation for Θ which can be solved numerically, for example by using the Newton method. The value of stress at the pole is then expressed from Eqs.(30) and (34),

$$p_0 = \frac{3R}{2r^2} \frac{\sin(\vartheta_R + \Theta)}{\cos^2(\vartheta_\mathrm{L} - \Theta)}. \tag{37}$$

The solution (Eqs.(36) and (37)) first appeared in (Ipavec (1999)). Due to the geometry of the articular sphere, the first choice of coordinates were spherical coordinates. In such coordinate system, the load - bearing area was subject to boundaries in which the two angles were related, so the load - bearing area had to be divided into 6 segments with different types of boundary shapes. Although yielding the same relatively simple result (Eq.(36)), the calculation was tedious and due to many terms in the integrals the probability of making the mistake was

increased. The derivation of the result was practically inaccessible by simply following the instructions given in (Ipavec (1999)). Probably this added to the fact that a typing mistake in the equations in (Ipavec (1999)) was deleterious for potential users of the model. The authors are indebted to W. Wilson and B.V. Rietbergen from Eindhoven University of Technology, who found the mistake while they were trying to repeat the derivation. An erratum was published in J. Biomech. (Ipavec (2002)), however, a thorough description of the model is still required as to help the potential users of the model to verify all steps.

In attempting to develop models with slightly more sophisticated load - bearing areas (such as after the Chiari osteotomy in which additional load - bearing area is created by a roof created by the cut iliac bone) the spherical coordinates used in (Ipavec (1999)) were found of practically no use and finding a more convenient coordinate system was prerequisite for description of the system. The coordinates presented above yielded considerably simpler derivation which was then first published in (Herman (2002)).

It can be seen that the simple, transparent and almost analytical form of the system of equations (35) - (37) does not mean that the model and the derivation of equations are simple. The simplicity and elegance of the result is primarily a consequence of the symmetry of the load - bearing area and of the stress distribution function.

It can also be mentioned that another choice of configuration preceded the above models. Inspired by Brinckmann et al., (Brinckmann (1981)), we chose the configuration in which the system was rotated so that the resultant hip force would point in the vertical direction (Iglič (1993b)). This model was however restricted to resultant hip force lying in the frontal plane of the body. It was a major achievement of the improved model described in (Ipavec (1999)) that regardless of the direction of the resultant hip force, within the described model, a coordinate system can always be found in which the above defined load-bearing area is symmetric.

To assess contact hip stress by a single numerical value, peak stress on the load - bearing area $p_{\max}$ is given. If the stress pole is located inside the load - bearing area, $p_{\max}$ is equal to the value of stress at the pole p_0. If the stress pole lies outside the load - bearing area, contact stress is the highest at the point of the load - bearing area which is closest to the stress pole and can be determined by using Eq.(5).

$$p_{\max} = p_0 \cos(\vartheta_L - \Theta). \tag{38}$$

2.2 Index of the hip stress gradient and functional angle of load-bearing area

Not only stress, but also stress differences between adjacent cell layers can be important in development of tissues (Daniel (2003)). These differences are expressed by the stress gradient,

$$\nabla p = \left(\frac{\partial p}{\partial r}, \frac{1}{r}\frac{\partial p}{\partial \theta}, \frac{1}{r \sin\theta}\frac{\partial p}{\partial \phi}\right) \tag{39}$$

where r is the magnitude of the radius vector while θ and ϕ are the polar and the azimuthal coordinates of the spherical system (Fig.3).

In this system

$$x = r \cos\phi \sin\theta, \tag{40}$$

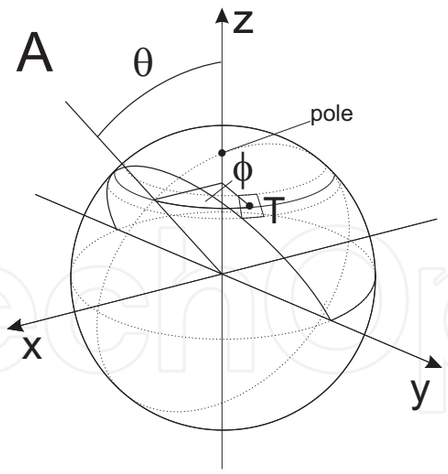

Fig. 3. Schematic presentation of the articular sphere in the spherical coordinate system.

$$y = r \sin\phi \sin\theta \tag{41}$$

and

$$z = r \cos\theta, \tag{42}$$

while the coordinates of the pole are

$$x_{\mathrm{p}} = r \cos\phi_{\mathrm{p}} \sin\theta_{\mathrm{p}}, \tag{43}$$

$$y_{\mathrm{p}} = r \sin\phi_{\mathrm{p}} \sin\theta_{\mathrm{p}} \tag{44}$$

and

$$z_{\mathrm{p}} = r \cos\theta_{\mathrm{p}}. \tag{45}$$

The space angle derived from the dot product is

$$\cos\gamma = \cos\theta \sin\phi \cos\phi_{\mathrm{p}} \sin\theta_{\mathrm{p}} + \sin\phi \sin\theta \sin\phi_{\mathrm{p}} \sin\theta_{\mathrm{p}} + \cos\theta \cos\theta_{\mathrm{p}}. \tag{46}$$

As in the rotated system the stress pole is at the top of the sphere, $\tilde{\theta}_{\mathrm{p}} = \tilde{\phi}_{\mathrm{p}} = 0$, the above expression simplifies into

$$\cos\gamma = \cos\theta. \tag{47}$$

It follows from Eqs.(39) and (47) that the gradient is

$$\nabla p = (0, -\frac{p_0}{r} \sin\theta, 0). \tag{48}$$

Here, r is the radius of the articular sphere. The stress gradient is a vector pointing in the direction of strongest change of stress. It would however be convenient to assess the gradient by a single numerical value. By mapping the three dimensional problem onto two dimensions we introduced the index of the hip stress gradient at the lateral acetabular rim G_p (Daniel (2002); Pompe (2003)),

$$G_p = -\frac{p_0}{r} \sin(\vartheta_{\mathrm{L}} - \Theta). \tag{49}$$

The absolute value of G_p is equal to the magnitude of stress gradient ∇p at the lateral acetabular rim. If the pole of stress distribution lies outside the load - bearing area (i.e., if

$\Theta > \vartheta_L$) then $G_p > 0$. If the pole of stress distribution lies inside the load - bearing area (i.e., if $\Theta < \vartheta_L$) then $G_p < 0$.

We defined another biomechanical parameter which describes the size of the load - bearing area: the functional angle ϑ_F. The functional angle is equal to the load - bearing area divided by $2r^2$,

$$\vartheta_F = \frac{\pi}{2} + \vartheta_{CE} - \Theta. \tag{50}$$

The index of the hip stress gradient at the lateral acetabular rim G_p is in a simple way connected to the size of the load-bearing area which is proportional to the functional angle of the load-bearing area,

$$G_p = \frac{p_0}{r} \cos \vartheta_F. \tag{51}$$

2.3 Clinical relevance of hip stress with respect to osteoarthritis development

Population studies have shown that long lasting high peak stress is unfavorable and leads to osteoarthritis of the hip, however, even if the peak stress is not very high, large positive index of the hip stress gradient at the lateral acetabular rim and small functional angle of the load - bearing area express unfavorable stress distribution.

Index of the hip stress gradient at the lateral acetabular rim G_p characterizes the slope of the contact stress distribution at the lateral border of the load - bearing area while the functional angle of the load-bearing area ϑ_F describes the amount of the articular sphere occupied by the load - bearing area. To illustrate these parameters Fig.4 presents stress distribution and parameter ϑ_F in two hips with different pelvic geometry: normal hip (A) and dysplastic hip (B). In hip A the pole of stress distribution lies within the load - bearing area and contact stress increases from the lateral edge in the medial direction, reaches its maximum and then decreases towards the medial border of the load - bearing area. The corresponding value of G_p is negative and the functional angle of the load - bearing area ϑ_F is large. In hip B the pole lies outside the load - bearing area so that at the lateral edge of the load - bearing area stress steeply decreases in the medial direction. The corresponding value of G_p is positive and the functional angle of the load - bearing area ϑ_F is small. The lower (more negative) the index of gradient and the larger the functional angle of the load - bearing area, the more favorable is stress distribution. In a population study it was shown (Pompe (2003)) that the change of sign of G_p correlates well with clinical evaluation of hip dysplasia, i.e. positive values of G_p correspond to dysplastic hips. The functional angle of the load-bearing area ϑ_F which does not critically depend on the size of the pelvis and femur was proved the most relevant in samples with large scattering in the size of the geometrical parameters, as for example in a group of children (Vengust (2001)) or if there is a possibility that the magnification of radiographs varies considerably. In these cases the effect of the parameters R, p_{max} and G_p (strongly dependent on the magnification of radiographs) can not be envisaged due to large scattering and concomitant poor statistical significance.

Population studies have shown that in dysplastic hips, the peak stress is on the average for a factor 2 higher than in healthy hips (Mavčič (2002)) while the index of stress gradient at the lateral acetabular rim is negative in normal hips and positive in dysplastic hips (Pompe (2003)). The differences were statistically significant ($p < 0.001$). In a study including 65 hips

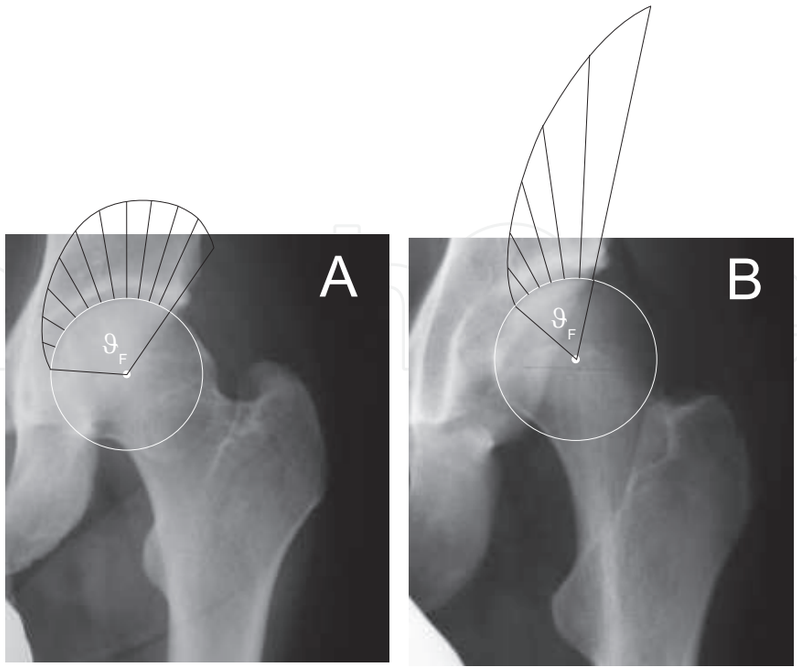

Fig. 4. Stress distribution in a frontal plane through the centre of the femoral head. The length of the line indicates the value of stress. The functional angle of the load - bearing area is shown. A: normal hip, B: dysplastic hip.

that underwent total hip replacement due to idiopathic osteoarthritis of the hip, the age at the replacement negatively correlated with peak stress ($p < 0.001$) (Rečnik (2009a)). These results indicate that contact hip stress plays an important role in progression of osteoarthritis.

3. Hip stress as etiological factor for avascular necrosis of femoral head

3.1 Introduction

Avascular necrosis of the femoral head (AN) is characterized by deterioration of the bone tissue (Figs.5,6). It represents together with secondary osteoarthritis a serious orthopaedic problem affecting mostly young and middle - aged populations (Mont (1995)). In spite of numerous studies, mechanisms leading to ischemic and necrotic processes are not yet understood. In about one third of patients the risk factors cannot be determined (Mahoney (2005)) while disorders and risk factors connected to the onset of AN include alcoholism (Mont (1995)), corticosteroid therapy in patients with connective tissue diseases and transplants (Mont (1995)), sickle cell anemia (Herndon (1972)), HIV (Miller (2002); Mahoney (2005)), antiphospholipid syndrome (Tektonidou (2003)) pregnancy (Cheng (1982); Mahoney (2005)) and some others (Bolland (2004); Macdonald (2001); Rollot (2005)). It was suggested that recidivant microfractures in the region of highly loaded femoral head may lead to microvascular trauma and thereby induce development of AN (Kim (2000)). A question can therefore be posed whether biomechanical parameters such as stresses in the hip are important in the onset of AN. It is the aim of this work to investigate the role of the above biomechanical parameters in the onset of AN.

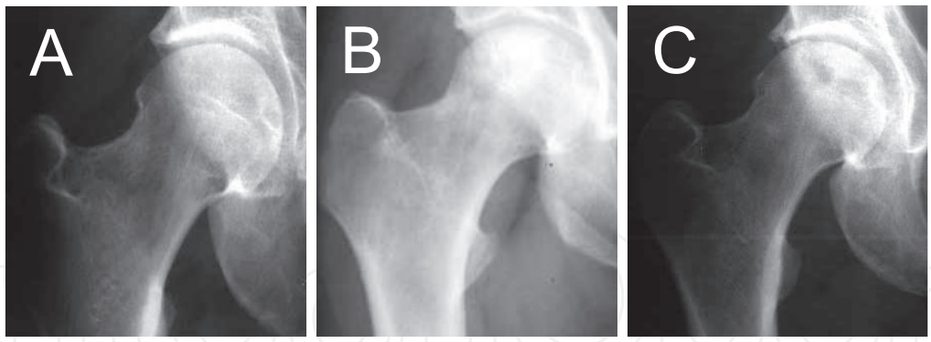

Fig. 5. A: healthy hip, B: initial phase of avascular necrosis of the femoral head when the femoral head is still spherical, C: advanced phase of avascular necrosis of the femoral head in which the femoral head is deformed while the femoral head is unable to bear load.

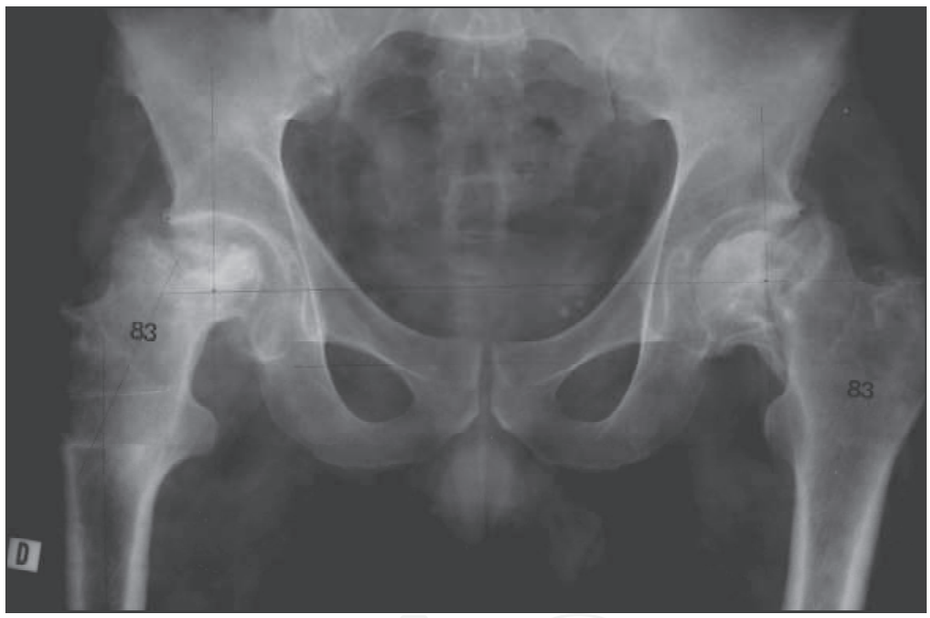

Fig. 6. Bilateral necrosis of the femoral head in an advanced stage.

3.2 Methods

From the archive of the Department of Orthopaedic Surgery, Ljubljana University Medical Centre we selected standard anterior - posterior radiograms of pelvis and proximal femora of 32 adult male persons (32 hips) who were treated due to AN between 1972 and 1991. It was assumed that prior to necrosis both hips had had the same geometry. As the necrotic process had already caused changes in the geometry of some hips, the hips contralateral to the necrotic ones were considered in the study. For comparison, we selected radiograms of 23 male persons (46 normal hips) pertaining to patients who had had a radiogram of the pelvic region taken at the same institution for reasons other than hip joint disease (e.g. lumbalgia). In our study we have considered only male hips. As the values of peak hip stress importantly depend on the gender (Kersnič (1997)) it is important to have gender-matched groups in statistical analysis.

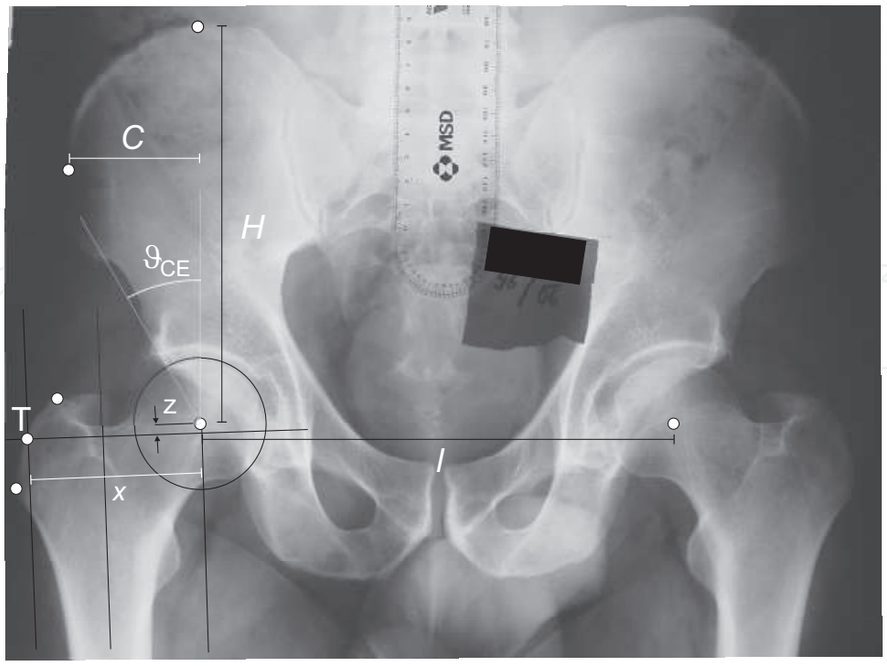

Fig. 7. Geometrical parameters of hip and pelvis which are needed to determine the resultant hip force within the HIPSTRESS method.

The three-dimensional biomechanical model for resultant hip force (Iglič (1993a)) and the above described model for hip stress were used to estimate the magnitude of the resultant hip force in the representative body position (one - legged stance) (Debevec (2010)). The contact stress distribution was given by its peak value $p_{\max}$, location of its pole Θ, index of the contact stress gradient at the lateral acetabular rim G_{p} and functional angle of the load - bearing area ϑ_{F}. The input parameters of the model for the resultant hip force are geometrical parameters of the hip and pelvis: interhip distance l, pelvic height H, pelvic width laterally from the femoral head center C and coordinates of the effective insertion point of abductors on the greater trochanter (point coordinates T_x, T_z) in the frontal plane (Fig.7).

The model of the resultant hip force is based on the equilibria of forces and torques acting between the body segments. To calculate the resultant hip force the three-dimensional reference coordinates of the muscle attachment points were taken from the work of Dostal and Andrews (Dostal (1981)) and scaled with regard to the pelvic parameters (l, C, H, T_x, T_z). To calculate stress, additionally, the radius of the articular surface (taken as the radius of the femoral head) and the angle of the lateral coverage of the femoral head (taken as the centre - edge angle of Wiberg $\vartheta_{\mathrm{L}} \equiv \vartheta_{\mathrm{CE}}$) were assessed from anterior - posterior radiograms for each individual subject. In some radiograms of the patients with AN the upper part of the pelvis was not visible. In these patients the contour was extrapolated on the basis of the visible parts. As in some hips with AN the femoral head was considerably flattened superiorly, centers of rotation on both sides corresponding to the pre - necrotic situation were determined by circles fitting the outlines of the acetabular shells.

To describe stress distribution, we determined biomechanical parameters R, $p_{\max}$, G_p and ϑ_{F} for each hip. The parameters $R, p_{\max}$ and G_p were normalized to the body weight (W_{B})

to outline the influence of hip geometry on stress. The respective average values in the test group and the control group were compared by the pooled two - sided Student t - test.

3.3 Results

Parameter (SD)	Test group	Control group	Δ (%)	p
ϑ_F [degrees]	105 (13)	113 (13)	7	0.008
Θ [degrees]	15.4 (7.2)	11.8 (7.6)	27	0.037
G_p/W_B [10^3 m^{-3}]	-17.32 (17.16)	-26.05 (16.85)	40	0.028
p_{max}/W_B [m^{-2}]	2172 (785)	2090 (502)	4	0.604
R/W_B	2.49 (0.21)	2.53 (0.18)	2	0.382

Table 1. Mean biomechanical parameters with standard deviation in brackets in the test group (32 hips contralateral to the necrotic hips) and in the control group (46 normal hips).

Table 1 shows the biomechanical parameters: functional angle of the load bearing area ϑ_F, position of the stress pole, normalized index of the contact stress gradient (G_p/W_B), normalized peak stress (p_{max}/W_B) and normalized resultant hip force (R/W_B) in the test group and in the control group. Hips in the test group are on average less favorable with respect to ϑ_F, G_p/W_B and p_{max}/W_B. The differences in ϑ_F (7%), Θ (27%) and G_p/W_B (40%) are statistically significant (p = 0.008, p = 0.037 and p = 0.028, respectively) while the difference in p_{max}/W_B (4%) is not statistically significant (p = 0.604). The magnitude of the resultant hip force R is smaller (more favorable) in the test group, however the difference is very small (2%) and statistically insignificant (p = 0.382).

Parameter (SD)	Test group	Control group	Δ (%)	p
C [mm]	60.0 (10.0)	58.5 (8.6)	3	0.463
H [mm]	163.0 (19.6)	162.4 (9.8)	0.4	0.867
l [mm]	203.1 (17.5)	199.6 (8.9)	2	0.305
T_x [mm]	12.5 (7.6)	7.6 (6.4)	49	0.002
T_z [mm]	74.7 (11.3)	69.7 (7.7)	7	0.033
r [mm]	28.5 (3.1)	27.7 (1.7)	3	0.187
ϑ_{CE}[degrees]	30.4 (5.6)	34.7 (6.1)	13	0.002

Table 2. Mean geometrical parameters with standard deviation in brackets in the test group (32 hips contralateral to the necrotic hips) and in the control group (46 normal hips).

In order to better understand the differences in biomechanical parameters, the differences in geometrical parameters used in the models for the above biomechanical parameters were studied (Table 2). The center-edge angle ϑ_{CE} is smaller (less favorable) in the test group than in the control group, the difference (13%) is statistically significant (p = 0.002). The lateral position of the insertion point of the effective muscle on the greater trochanter (T_z) is statistically significantly more favorable in the test group than in the control group (p = 0.033), while its inferior position (T_x) is considerably (49%) and statistically significantly more favorable in the control group (p = 0.002). The differences in other geometrical parameters are small and statistically insignificant.

3.4 Discussion

Our results show that the peak contact hip stress $p_{\max}/W_B$ in the group of hips contralateral to necrotic ones and in the group of normal hips are not statistically significantly different, however, the shape of the stress distribution (given by parameters ϑ_F and G_p/W_B) is statistically significantly less favorable in the group of hips contralateral to necrotic ones.

The differences in the biomechanical parameters can be explained by the differences in the geometrical parameters. The difference in pelvic height H and width C and in the interhip distance l were very small (below 3%) and statistically insignificant while the difference in the vertical coordinate of the insertion of the effective muscle on the greater trochanter (T_x) was statistically significant, but this parameter does not influence much the biomechanical parameters (Daniel (2001)). The differences in the remaining three parameters (lateral coordinate of the insertion of the effective muscle on the greater trochanter, radius of the femoral head and center-edge angle) can however contribute to the explanation of the differences in biomechanical parameters. The centre - edge angle CE is the most important parameter in determination of contact stress distribution. Larger CE corresponds to lower $p_{\max}/W_B$ and smaller G_p/W_B. Table 2 shows that ϑ_{CE} is statistically significantly lower in the test group (p = 0.002) indicating that $p_{\max}/W_B$ and G_p/W_B would be higher in hips contralateral to the necrotic ones. However, $p_{\max}/W_B$ and G_p/W_B strongly depend also on the radius of the femoral head ($p_{\max}/W_B$ is inversely proportional to the square of r and G_p/W_B is inversely proportional to the third power of r). Although the difference in the radii of the two groups is not statistically significant (p = 0.187), the difference (3%) is in favor of hips in the test group. Further, the lateral position of the insertion of the effective muscle is for 7% statistically significantly larger (more favorable) in the test group than in the control group (p = 0.002). The effect of the smaller center-edge angle is therefore counterbalanced by the effect of larger femoral head and more laterally extended greater trochanter. The shape of the stress distribution (described by ϑ_F and G_p/W_B) is on average considerably and statistically significantly different in both groups. In the test group the distribution is steeper, the pole lies more laterally, the gradient index is larger (less negative) and the functional angle of the load-bearing area is smaller than in the control group. This renders hips with increased risk for AN less favorable regarding the stress distribution. However, we did not find a statistically significant difference in $p_{\max}/W_B$.

The magnification of the radiograph was not known, as no unit with known length was visible in the picture. As the magnification may vary considerably contributing to the scattering in the measured distances, poor statistical significance in parameters $p_{\max}/W_B$ and R/W_B can be the consequence of the lack of knowledge of magnification of the radiograms.

It has been hypothesized that transient osteoporosis of the bone marrow oedema syndrome may be the initial phase of osteonecrosis of the femoral head (Hofmann (1994)) and that there may be a common patophysiology. Transient osteoporosis is connected to recidivant microfractures and microvascular trauma at highly loaded regions of the bone leading to the ishemia of the affected part of the bone (Ficat (1981)). Higher contact hip stress may increase the probability and extent of microfractures of the affected bone thereby making the repair more difficult. Furthermore, the replicative capacity of osteoblast cells of the intertrochanteric area of the femur in osteonecrosis patients was found to be significantly reduced compared to

patients with osteoarthritis (Gangji (2003)). Thereby, stresses in the hip including the contact hip stress could contribute to the acceleration of the processes leading to AN.

4. Conclusion

Unfavorable stress distribution importantly influences development of the hip and may present a risk factor for osteoarthritis progression as well as for progression of the avascular necrosis of the femoral head.

5. Acknowledgement

Authors are indebted to A. Iglič for discussions and to R. Štukelj and L. Drobne for technical assistance.

6. References

Bolland, M.J., Hood, G., Bastin, S.T., King, A.R., Grey, A., (2004). Bilateral femoral head osteonecrosis after septic shock and multiorgan failure. *J Bone Min Res*, 19, (517-520), ISSN 0884-0431

Brand, R.A., Iglič, A., Kralj-Iglič, V., (2001). Contact stresses in human hip: implications for disease and treatment. *Hip Int*, 11, (117-126), ISSN 1120-7000

Brinckmann, P., Frobin, W., Hierholzer, E.,(1981). Stress on the articular surface of the hip joint in healthy adults and persons with idiopathic osteoarthrosis of the hip joint. *J Biomech*, 14, (149-156), ISSN 0044-3220

Cheng, N., Burssens, A., Mulier, J.C., (1982). Pregnancy and post-pregnancy avascular necrosis of the femoral head. *Arch Orthop Trauma Surg*, 100, (199-210), ISSN 0936-8051

Daniel, M., Antolič, V., Iglič, A., Kralj Iglič., V., (2001). Determination of contact hip stress from nomograms based on mathematical model. *Med Eng Phys*, 23, (347-357), ISSN 1350-4533

Daniel, M., Sochor, M., Iglič, A., Herman, S., Kralj-Iglič, V., (2002). Gradient of contact stress in normal and dyplastic human hips. *Acta Bioeng Biomech, Suppl.* 1, (280-281), ISSN 1509409X

Daniel, M., Sochor, M., Iglič, A., Kralj-Iglič, V., (2003). Hypothesis of regulation of hip joint cartilage activity by mechanical loading. *Medical Hypotheses*, 60, (936-937), ISSN 0306-9877

Daniel, M., Dolinar, D., Herman, S., Sochor, M., Iglič, A., Kralj-Iglič, V., (2006). Contact stress in hips with osteonecrosis of the femoral head. *Clin Orhop Rel Res*, 447, (92-99), ISSN 0009-921X

Daniel, M., Iglič A., Kralj - Iglič, V., (2011). Human hip joint loading - mathematical modeling.Reaction forces and contact pressures. *VDM Verlag Dr. Müller e.K.*, ISBN 978-3-639-26120-2

Debevec, H., Pedersen, D. R., Iglič, A., Daniel, M. (2010). One-legged stance as a representative static body position for calculation of hip contact stress distribution in clinical studies *J Appl Biomech* , ISSN 1065-8483

Dolinar, D., Antolič, V., Herman, S., Iglič, A., Kralj-Iglič, V., Pavlovčič, V., (2003). Influence of contact hip stress on the outcome of surgical treatment of hips affected by avascular necrosis. *Arch Orthop Trauma Surg*, 123, (509-513), ISSN 0936-8051

Dostal, W.F., Andrews, J.G., (1981). A three-dimensional biomechanical model of the hip musculature. *J Biomech*, 14, (803-812), ISSN 0021-9290

Eberhardt, A.W., Lewis, J.L., Keer, L.M., (1991). Contact of layered elastic spheres as a model of joint contact: effect of tangential load and friction. *J Biomech Eng*, 113, (107-108), ISSN 0148-0731

Ficat RP, Arlett, J., (1981). Functional investigation of bone under normal conditions. In: Hungerford, D.S., (ed): Ishemia and necrosis of bone. Baltimore, Williams and Wilkins; 29-52.

Gangji, V., Hauzeur, J.P., Schoutens, A., Hinsenkamp, M., Appelboom, T., Egrise, D., (2003). Abnormalities in the replicative capacity of osteoblastic cells in the proximal femur of patients with osteonecrosis of the femoral head. *J Rheumatol*, 30, (348-351), ISSN 0884-0431

Herman, S., Jaklič, A., Herman, S., Iglič A., Kralj-Iglič, V., (2002). Hip stress reduction after Chiari osteotomy. *Med Biol Eng Comput*, 40, (369-375), ISSN 0009-921X

Herndon, J.H., Aufranc, O.E., (1972). Avascular necrosis of femoral head in the adult. A review of its incidence in a variety of conditions. *Clin Orthop Rel Res*, 86, (43-62), ISSN 0009-921X

Hofmann, S., Engel, A., Neuhold, A., Leder, K., Kramer, J., Plenk, H. Jr., (1994). Bone-marrow oedema syndrome and transient osteoporosis of the hip. An MRI-controlled study of treatment by core decompression. *J Bone Joint Surg*, 76-B, (993-994) ISSN 0301-620X

Iglič, A., Srakar, F., Antolič ,V., Kralj-Iglič, V., Batagelj, V., (1990). Mathematical analysis of Chiari osteotomy. *Acta Orthop Iugosl*, 20, (35-39), ISSN 0350-2309

Iglič, A., Srakar, F., Antolič, V., (1993). Influence of the pelvic shape on the biomechanical status of the hip. *Clin Biomech*, 8, (223-224), ISSN 0268-0033

Iglič, A., Kralj-Iglič, V., Antolič, V., Srakar, F., Stanič, U.,(1993). Effect of the periacetabular osteotomy on the stress on the human hip joint articular surgace. *IEEE T Rehabil Eng*, 1, (207-212), ISSN 1063-6528

Ipavec, M., Brand, R.A., Pedersen, D.R., Mavčič, B., Kralj-Iglič, V., Iglič, A., (1999). Mathematical modelling of stress in the hip during gait. *J Biomech*, 32, (1229-1235), ISSN 0021-9290

Ipavec, M., Brand, R.A., Pedersen, D.R., Mavčič, B., Kralj-Iglič, V., Iglič, A., (2002). Erratum to: Mathematical modelling of stress in the hip during gait, [Journal of Biomechanics, 32(11) (1999) 1229-1235]. *J Biomech*, 35, (555), ISSN 0021-9290

Kersnič, B., Iglič, A., Kralj-Iglič, V., Srakar, F., Antolič, V., (1997). Increased incidence of arthrosis in female population could be related to femoral and pelvic shape. *Arch Orthop Trauma Surg*, 116, (345-347), ISSN 0936-8051

Kim, Y.M., Oh, H.C., Kim, H.J., (2000). The pattern of bone marrow oedema on MRI in osteonecrosis of the femoral head. *J Bone Joint Surg*, 82-B, (837-841), ISSN 0301-620X

Miller, K.D., Masur, H., Jones, E.C. et al., (2002). High prevalence of osteonecrosis of the femoral head in HIV infected adults. *Ann Intern Med*, 137, (17-25), ISSN 0003-4819

Kralj, M., Mavčič, B., Antolič, V., Iglič, A., Kralj-Iglič, V., (2005). The Bernese periacetabular osteotomy: clinical, radiographic and biomechanical 7-15 year follow-up in 26 hips. *Acta Orthop*, 76, (833-840), ISSN 1745-3674

Lipshitz, H., Glimcher, M.J., (1979). In vitro studies of the wear of articular cartilage. II Characteristics of the wear of articular cartilage when worn against stainless steel plates having characteristic surfaces. *Wear*, 52, (297-339), ISSN 0043-1648

Macdonald, A.G., Bissett, J.D., (2001). Avascular necrosis of the femoral head in patients with prostate cancer treated with cyproterone acetate and radiotherapy. *Clin Oncol*, 13, (135-137), ISSN 0936-6555

Mahoney, C.R., Glesby, M.J., DiCarlo, E.F., Peterson, M.G., Bostrom, M.P. (2005). Total hip arthroplasty in patients with human immunodeficiency virus infection: pathologic findings and surgical outcomes. *Acta Orthop*, 76, (198-203), ISSN 1745-3674

Mavčič, B., Pompe, B., Antolič, V., Daniel, M., Iglič, A., Kralj-Iglič, V., (2002). Mathematical estimation of stress distribution in normal and dysplastic human hips. *J Orthop Res*, 20, (1025-1030), ISSN 0736-0266

Mavčič, B., Iglič, A., Kralj-Iglič, V., Brand, R.A., Vengust, R., (2008). Cumulative hip contact stress predicts osteoarthritis in DDH. *Clin Orthop Rel Res*, 466, (884-891), ISSN 0009-921X

McCutchen, C.W., (1962). The frictional properties of animal joints. *Wear*, 5, (1-17), ISSN 0043-1648.

Mont, M.A., Hungerford, D.S. (1995). Non-traumatic avascular necrosis of the femoral head. *J Bone Joint Surg*, 77-A, (459-469), ISSN 0021-9355

Pompe, B., Daniel, M., Sochor, M., Vengust, R., Kralj-Iglič, V., Iglič, A., (2003). Gradient of contact stress in normal and dysplastic human hips. *Med Eng Phys*, 25, (379-385), ISSN 1350-4533

Pompe, B., Antolič, V., Mavčič, B., Iglič, A., Kralj-Iglič, V., (2007). Hip joint contact stress as an additional parameter for determining hip dysplasia in adults: Comparison with Severin's classification. *Med Sci Monitor*, 13,(CR215-219), ISSN 1234-1010

Rečnik, G., Kralj-Iglič ,V., Iglič, A., Antolič,V., Kramberger, S., Vengust, R., (2007). Higher peak contact hip stress predetermines the side of hip involved in idiopathic osteoarthritis. *Clin Biomech*, 22, (1119-1124), ISSN 0268-0033

Rečnik, G., Vengust, R., Kralj-Iglič, V., Vogrin, M., Kranjc Z., Kramberger, S., (2009). Association between Sub-clinical acetabular dysplasia and a younger age at hip arthroplasty in idiopathic osteoarthritis. *J Int Med Res*, 37, (1620-1625) ISSN 0300-0605

Rečnik, G., Kralj-Iglič, V., Iglič, A., Antolič, V., Kramberger, S. , Rigler, I., Pompe, B., Vengust, R., (2009). The role of obesity, biomechanical constitution of the pelvis and contact joint stress in progression of hip osteoarthritis. *Osteoarthr Cartilage*, 3, (879-882), ISSN 1063-4584

Rollot, F., Wechsler, B., du Boutin, le T.H., De Gennes, C., Amoura, Z., Hachulla, E., Piette, J.C., (2005). Hemochromatosis and femoral head aseptic osteonecrosis: a nonfortuitous association. *J Rheumatol*, 32, (376-378), ISSN 0315-162X

Tektonidou, M.G., Malagari, K., Vlachoyiannopoulos, P.G., Kelekis, D.A., Moutsopoulos, H.M., (2003). Asymptomatic avascular necrosis in patients with primary antiphospholipid syndrome in the absence of corticosteroid use: A prospective study by magnetic resonance imaging. *Arthritis Rheum*, 48, (732-736), ISSN 0004-3591

Vengust, R., Daniel, M., Antolič, V., Zupanc, O., Iglič, A., Kralj-Iglič, V., (2001). Biomechanical evaluation of hip joint after Salter innominate osteotomy: a long-term follow-up study. *Arch Orthop Trauma Surg*, 121, (511-516), ISSN 0936-8051

Zupanc, O., Križančič, M., Daniel, M., Mavčič, B., Antolič, V., Iglič, A., Kralj-Iglič, V., (2008). shear stress in epiphyseal growth plate is a risk factor for slipped capital femoral epiphysis. *J Pediatr Orthoped*, 28, (444-451), ISSN 0271-6798

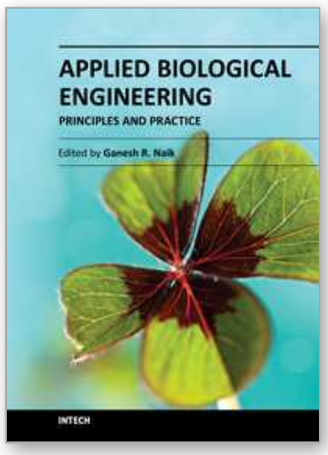

Applied Biological Engineering - Principles and Practice
Edited by Dr. Ganesh R. Naik

ISBN 978-953-51-0412-4
Hard cover, 662 pages
Publisher InTech
Published online 23, March, 2012
Published in print edition March, 2012

Biological engineering is a field of engineering in which the emphasis is on life and life-sustaining systems. Biological engineering is an emerging discipline that encompasses engineering theory and practice connected to and derived from the science of biology. The most important trend in biological engineering is the dynamic range of scales at which biotechnology is now able to integrate with biological processes. An explosion in micro/nanoscale technology is allowing the manufacture of nanoparticles for drug delivery into cells, miniaturized implantable microsensors for medical diagnostics, and micro-engineered robots for on-board tissue repairs. This book aims to provide an updated overview of the recent developments in biological engineering from diverse aspects and various applications in clinical and experimental research.

InTech Europe
University Campus STeP Ri
Slavka Krautzeka 83/A
51000 Rijeka, Croatia
Phone: +385 (51) 770 447
Fax: +385 (51) 686 166
www.intechopen.com

InTech China
Unit 405, Office Block, Hotel Equatorial Shanghai
No.65, Yan An Road (West), Shanghai, 200040, China
中国上海市延安西路65号上海国际贵都大饭店办公楼405单元
Phone: +86-21-62489820
Fax: +86-21-62489821

IntechOpen